JACS
JOURNAL OF THE AMERICAN CHEMICAL SOCIETY
pubs.acs.org/JACS
Communication

High-Mobility Flexible Oxyselenide Thin-Film Transistors Prepared by a Solution-Assisted Method

Congcong Zhang, Jinxiong Wu,* Yuanwei Sun, Congwei Tan, Tianran Li, Teng Tu, Yichi Zhang, Yan Liang, Xuehan Zhou, Peng Gao, and Hailin Peng*

Cite This: J. Am. Chem. Soc. 2020, 142, 2726−2731
Read Online
ACCESS | Metrics & More | Article Recommendations | Supporting Information

ABSTRACT: Two-dimensional (2D) semiconductors hold great promise in flexible electronics because of their intrinsic flexibility and high electrical performance. However, the lack of facile synthetic and subsequent device fabrication approaches of high-mobility 2D semiconducting thin films still hinders their practical applications. Here, we developed a facile, rapid, and scalable solution-assisted method for the synthesis of a high-mobility semiconducting oxyselenide (Bi_2O_2Se) thin film by the selenization and decomposition of a precursor solution of $Bi(NO_3)_3{\cdot}5H_2O$. Simply by changing the rotation speed in spin-coating of the precursor solution, the thicknesses of Bi_2O_2Se thin films can be precisely controlled down to few atomic layers. The as-synthesized Bi_2O_2Se thin film exhibited a high Hall mobility of ~74 $cm^2\ V^{-1}\ s^{-1}$ at room temperature, which is much superior to other 2D thin-film semiconductors such as transition metal dichalcogenides. Remarkably, flexible top-gated Bi_2O_2Se transistors showed excellent electrical stability under repeated electrical measurements on flat and bent substrates. Furthermore, Bi_2O_2Se transistor devices on muscovite substrates can be readily transferred onto flexible polyvinyl chloride (PVC) substrates with the help of thermal release tape. The integration of a high-mobility thin-film semiconductor, excellent stability, and easy transfer onto flexible substrates make Bi_2O_2Se a competitive candidate for future flexible electronics.

High-mobility two-dimensional (2D) semiconductors, such as transition metal dichalcogenides (TMDCs), black phosphorus, InSe, and Bi_2O_2Se,[1−5] have attracted considerable attention in post-silicon electronics. In contrast to typical bulk semiconductors, the intrinsic atomic thickness of 2D semiconductors brings a lot of unprecedented characteristics and unique applications.[4,6−10] Except for much suppressed short channel effects in nanoscale transistors, the ultrathin body will also introduce excellent intrinsic flexibility and thus holds great promise for applications in flexible electronics such as flexible displays and integrated circuits.[11−14] At present, despite the existence of a large family of 2D semiconductors, the lack of simple synthetic approaches of high-mobility 2D semiconducting thin films and compatible device fabrication for flexible electronics still hinders their practical applications.[13,15−19] For example, continuous thin films of TMDCs (MoS_2) synthesized by chemical vapor deposition (CVD) or solution methods usually have relatively low mobility (<10 $cm^2\ V^{-1}\ s^{-1}$).[20−22] Additionally, devices on flexible substrates usually exhibit much lower performance than those on rigid substrates. The performance degradation is mainly attributed to drawbacks of flexible substrates, such as substrate cleanliness, limited process temperature, and strain induced by roughness.[23−25]

The pivotal part of the success of any materials in electronic applications is the development of a rapid, scalable, and facile process to synthesize high-quality thin films. In view of elemental components, Bi_2O_2Se can derive from its parent compound of Bi_2O_3 by partially replacing O by Se.[26] Hence, it is reasonable to determine whether Bi_2O_2Se can be obtained by selenization of Bi_2O_3, whose chemical reactions can be represented as follows: $Bi_2O_3 + Se_2(g) \rightarrow Bi_2O_2Se + SeO_2(g)$.

As shown in Figure 1a,b, we developed a two-step method to synthesize a Bi_2O_2Se thin film on flexible muscovite substrates, namely, depositing an ultrathin Bi_2O_3 film first, then selenizing Bi_2O_3 to get a Bi_2O_2Se thin film. First, large-area ultrathin Bi_2O_3 films were synthesized by a solution-assisted and spin-coating method. $Bi(NO_3)_3{\cdot}5H_2O$, a very cheap commercial reagent, was dissolved in ethylene glycol, then spin-coated onto a muscovite substrate at a certain rotation speed. Due to the excellent affinity between the solution and muscovite substrate, where the contact angle is as small as 6° (Figure S1), the $Bi(NO_3)_3$ solution spread out on the whole muscovite substrate with excellent uniformity. The nitrates on muscovite were then annealed in air to get uniform Bi_2O_3 thin films (Figures S2 and S3), whose thicknesses can be readily tailored by changing the rotation speed or the concentration of the Bi precursors. The decomposition reaction proceeded as follows: $Bi(NO_3)_3{\cdot}5H_2O \rightarrow Bi_2O_3 + NO_x(g) + O_2(g) + H_2O$.

Figure 1c shows the typical microscopic image of as-synthesized Bi_2O_2Se thin films on flexible muscovite substrates. As shown in Figure 1d and e, the identical contrast over a large scale indicates the excellent uniformity of the Bi_2O_2Se thin film, exhibiting a very smooth surface with a surface roughness

Received: November 5, 2019
Published: January 27, 2020

https://dx.doi.org/10.1021/jacs.9b11668
J. Am. Chem. Soc. 2020, 142, 2726−2731

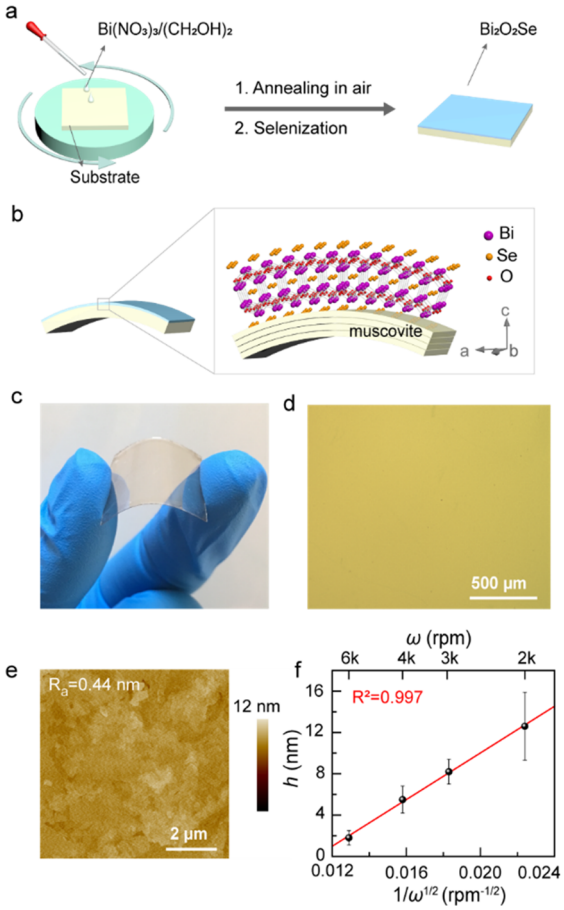

Figure 1. Schematic diagram and morphological characterization of a Bi_2O_2Se thin film prepared by a solution-assisted method. (a) Preparation process of the Bi_2O_2Se thin film, in which a $Bi(NO_3)_3/(CH_2OH)_2$ solution was first spin-coated on a muscovite substrate, followed by annealing in air and another step of selenization to obtain a Bi_2O_2Se thin film. (b) Diagram of a Bi_2O_2Se thin film on a bendable muscovite substrate, which facilities the fabrication of flexible electronics. (c) Photograph of an as-synthesized Bi_2O_2Se thin film on a flexible muscovite substrate (2 cm × 2 cm). (d) Typical optical microscope (OM) image of an as-synthesized Bi_2O_2Se thin film with excellent uniformity. (e) Typical AFM image of a Bi_2O_2Se thin film with a relatively small roughness (Ra = 0.44 nm). (f) Thickness (h) of the as-synthesized Bi_2O_2Se thin film as a function of $\omega^{-1/2}$.

as small as 0.44 nm measured by atomic force microscopy (AFM). Additionally, spin coating is a facile way to change the thickness of the as-prepared thin film by changing the rotation speed, as the function that follows:

$$h \propto \left(\frac{\mu}{t\omega}\right)^{1/2}$$

where h is the thickness of the obtained thin film, μ stands for the viscosity of the solution, t represents the time of rotation, and ω is the rotation speed. As shown in Figures 1f and S4, the thickness (h) of the as-synthesized Bi_2O_2Se thin film shows excellent linear dependence of $\omega^{-1/2}$, whose correlation coefficient is 0.997 (very close to 1). In other words, we can readily tailor the thickness of the as-synthesized Bi_2O_2Se thin film even down to a few atomic layers, which is quite challenging for the traditional CVD method with very complicated elementary steps.

To investigate the crystal structure and domain size of the as-synthesized Bi_2O_2Se thin film, we performed characterization by X-ray diffraction (XRD) and electron backscatter diffraction (EBSD). The as-synthesized Bi_2O_2Se thin film can be readily transferred onto a glass slide for XRD characterization via a poly(methyl methacrylate) (PMMA)-assisted method. As indicated in Figure 2a, the Bi_2O_2Se thin film

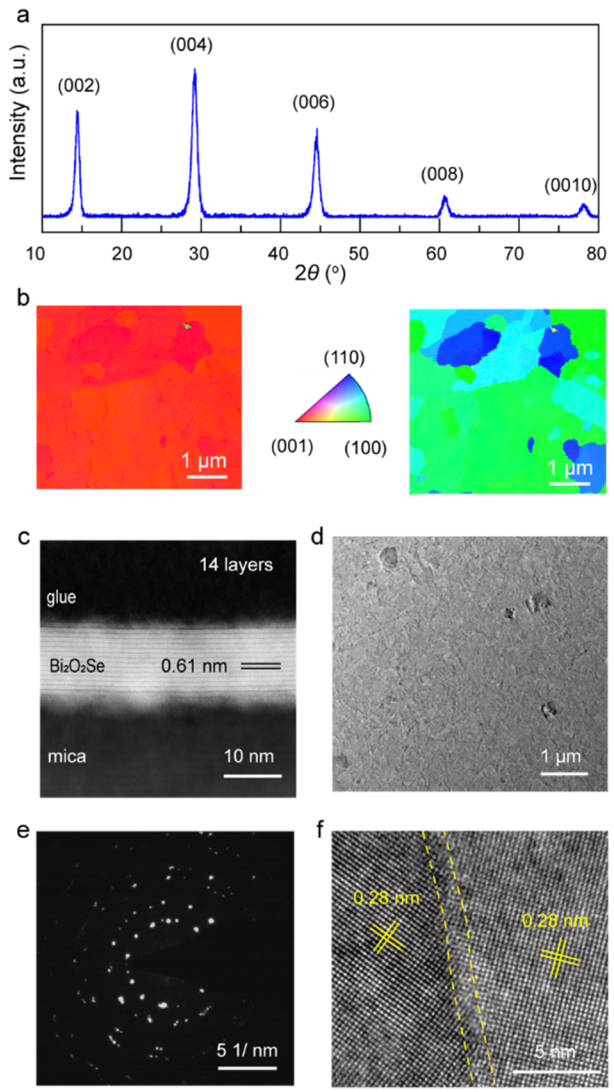

Figure 2. Structural characterization of a Bi_2O_2Se thin film prepared by a solution-assisted method. (a) XRD pattern of a Bi_2O_2Se thin film transferred onto a glass slide, showing only (001) indices. (b) EBSD patterns of a Bi_2O_2Se thin film on muscovite, showing a domain size from hundreds of nanometers to several micrometers. (c) Cross-sectional STEM image of a Bi_2O_2Se thin film on a muscovite substrate. (d) TEM image of a Bi_2O_2Se thin film transferred onto a Cu grid, whose zone axis is [001]. (e) Typical SAED pattern of a Bi_2O_2Se thin film with polycrystalline diffraction ring. (f) HRTEM of Bi_2O_2Se domains merged together with different in-plane orientations.

showed only (001) indices, suggesting all the composed Bi_2O_2Se domains adopted an "in-plane growth mode" (not vertical). The EBSD patterns of the Bi_2O_2Se thin film on muscovite are consistent with the XRD results, showing a domain size from hundreds of nanometers to several micrometers (Figure 2b). As we know, electrons flowing

https://dx.doi.org/10.1021/jacs.9b11668
J. Am. Chem. Soc. 2020, 142, 2726−2731

inside the layer usually dominate the electrical transport in a layered material. Therefore, the "in-plane growth mode" is typically preferable to keep high mobility for a layered thin film.

Cross-sectional scanning transmission electron microscopy (STEM) is a powerful tool for thin-film characterizations. As shown in Figure 2c, the as-synthesized Bi_2O_2Se thin film exhibits a typical layered structure, whose layer spacing of 0.61 nm is consistent with the theoretical value of the layer thickness in Bi_2O_2Se (0.608 nm). The film thickness is ~8.5 nm, which matches well with the AFM results (Figure S5). Additionally, we performed top-view transmission electron microscopy (TEM) characterizations of the as-synthesized Bi_2O_2Se thin film by transferring it onto a holey carbon supported Cu grid (Figure 2d–f). The typical selected area electron diffraction (SAED) pattern displayed several sets of diffraction patterns on a ring, suggesting the in-plane domain direction of Bi_2O_2Se is relatively random. To this end, a domain boundary will form when two domains with different crystal orientations merge together, which is clearly marked by the yellow dashed line in Figure 2f. The lattice spacing of 0.28 nm is identical to the theoretical value (0.27 nm) of lattice distance for the (110) plane in Bi_2O_2Se.

To evaluate the electrical properties of the as-synthesized Bi_2O_2Se thin film, we first patterned the Bi_2O_2Se continuous thin film (8 nm) into discrete 40 × 20 μm^2 sheets by a wet chemical etching method reported before[27] and then fabricated the sheets into standard Hall-bar devices (inset of Figure 3a).

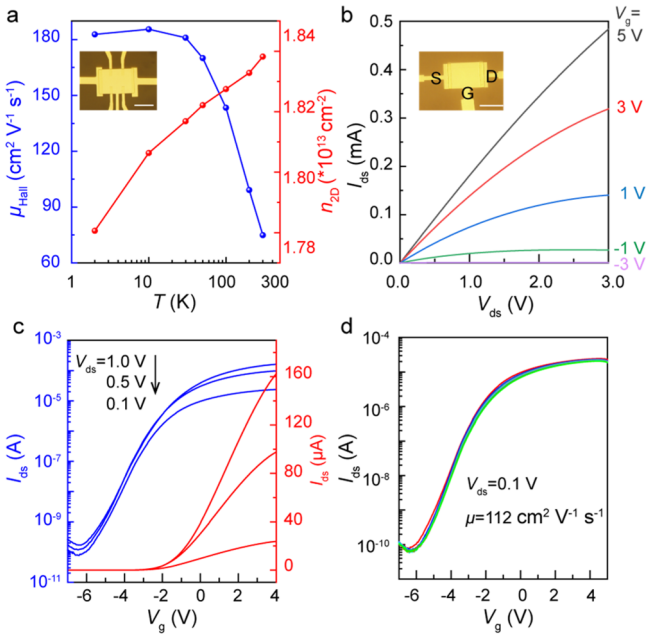

Figure 3. Electrical properties of a Bi_2O_2Se thin film prepared by a solution-assisted method. (a) Hall mobility (μ_{Hall}) and carrier concentration (n_{2D}) as a function of temperature in the Bi_2O_2Se thin film. Inset: OM image of a Hall-bar device fabricated on the 8 nm thick Bi_2O_2Se thin film. Scale bar, 20 μm. (b) Output curves obtained from an 8 nm thick Bi_2O_2Se transistor at room temperature. Inset: OM image of a top-gated device fabricated on a muscovite substrate, with Pd/Au electrodes and 20 nm HfO_2 serving as the top-gate dielectrics. (c) Transfer curves (I_{ds}–V_g) of the device with different source–drain voltages (1.0, 0.5, 0.1 V). (d) Repeating the transfer curve (V_{ds} = 0.1 V) tests 10 times, showing ignorable drift on threshold voltage and saturation current.

As shown in Figure 3a, the Hall mobility of an as-synthesized Bi_2O_2Se thin film can be as high as 74 cm^2 V^{-1} s^{-1} at room temperature and increases gradually upon cooling. It is worth noting that the room-temperature Hall mobility is much higher than other reported 2D semiconducting films and commercial InGaZnO thin films.[25,28−31] Besides, the high-mobility 2D Bi_2O_2Se thin films were fabricated into top-gated field-effect transistors. As shown in Figure 3b, the I_{ds}–V_{ds} shows a linear dependence at low drain–source biases, suggesting an ohmic contact was formed. Transfer curves (I_{ds}–V_g) of the device with different source–drain voltages (1.0, 0.5, 0.1 V) all exhibited a large on/off ratio of >10^5 (Figure 3c). By linear fitting of the transfer curves based on the equation $\mu_{app} = (L/W)(1/C_g)(dI_{ds}/dV_g)$, we can extract a two-probe apparent field-effect mobility as high as ~110 cm^2 V^{-1} s^{-1}. Electrical stability is another key parameter that determines whether a device can be put into practical applications or not,[32,33] since it is challenging to remove interfacial trap states, which will cause drain-induced barrier lowering (DIBL) under repeated transfer-curve measurements. Remarkably, the top-gated Bi_2O_2Se transistors showed ignorable drift on threshold voltage and saturation current (Figure 3d), which laid a solid foundation for practical applications that need excellent electrical stability, such as flexible electronics.

The feature of an ultrathin semiconducting film with intrinsic flexibility, excellent electrical stability, and high mobility in Bi_2O_2Se greatly facilitates its application in flexible electronics. As we know, because of the large surface roughness and incompatibility with the microfabrication process, it is very challenging to directly fabricate the devices on flexible polymer substrates, such as polyvinyl chloride (PVC). The preferable way is to fabricate the devices on a flat and rigid substrate first, then transfer the complete device onto other targeted flexible substrates, such as etching the sacrificial solid substrate.[24,34−36]

Thanks to the layered structure, the muscovite substrates can be easily exfoliated into thin flakes at any thickness with excellent flexibility (Figure 4a) and stacks closely onto a flexible polymer substrate, such as PVC, to investigate the electrical performance of flexible transistors under repeated bending tests. First, we transfer the complete Bi_2O_2Se top-gated devices with ultrathin muscovite substrates underneath onto a thermal release tape; then the devices can be released onto the polymer substrates just by ~100 °C heating (Figure S6). This facile transferring process greatly facilities the fabrication and electrical measurements of Bi_2O_2Se flexible transistors. Figure 4a demonstrates the diagram of a flexible Bi_2O_2Se transistor on muscovite/PVC substrates, and Figure 4b shows the devices with a curvature radius (R) of 4.0 mm. It is worth noting that drain current (I_{ds}) plotted against the gate voltage (V_g) shows a very slight change when the device is bent to 4.0, 5.3, and 7.8 mm (Figure 4c). Furthermore, the extracted field-effect mobilities of a flexible Bi_2O_2Se transistor bent at different curvature radii all have a similar value of ~100 cm^2 V^{-1} s^{-1} (Figure 4d). The transfer characteristics of flexible Bi_2O_2Se transistors and extracted mobilities also showed very slight changes after 0, 200, 400, ..., 1000 consecutive bending cycles at a 4.0 mm bending radius (Figure 4e,f). In a word, the Bi_2O_2Se thin films synthesized by a solution-assisted method showed excellent electrical stability when fabricated into flexible electronics.

In conclusion, high-mobility semiconducting Bi_2O_2Se thin films were successfully prepared by a rapid, scalable, and facile solution-assisted method. The precise control on the quantity

https://dx.doi.org/10.1021/jacs.9b11668
J. Am. Chem. Soc. 2020, 142, 2726−2731

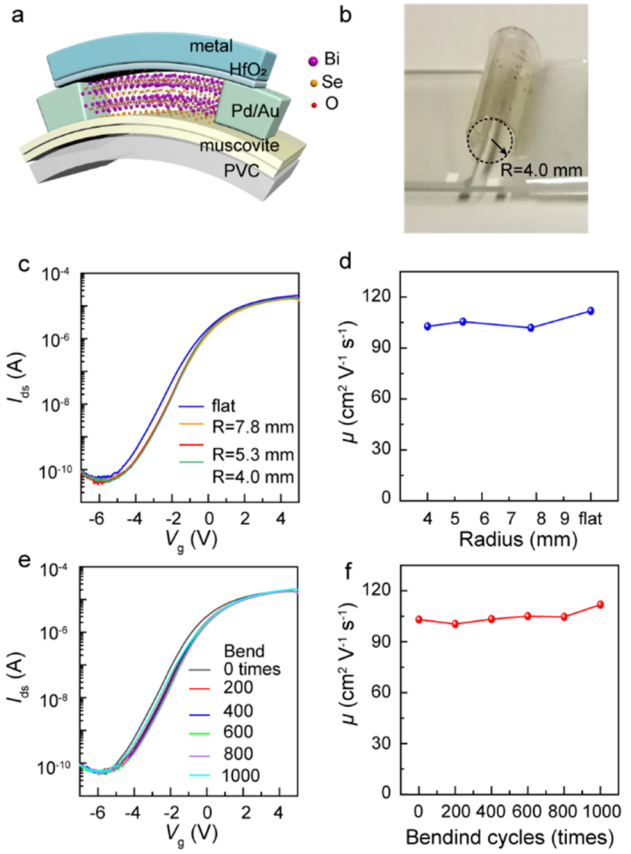

Figure 4. Electrical performance of a flexible Bi_2O_2Se transistors under repeated bending tests. (a) Device configuration of a flexible Bi_2O_2Se transistor on an ultrathin muscovite substrate with excellent flexibility. (b) Photograph of flexible Bi_2O_2Se transistors on a muscovite/PVC substrate with a curvature radius (R) of 4.0 mm. (c) Drain current plotted against the gate voltage (I_{ds}–V_g), showing a very slight change when the device is bent to 4.0, 5.3, and 7.8 mm. (d) Extracted field-effect mobilities of a flexible Bi_2O_2Se transistor bent at different curvature radii. (e) Transfer characteristics of flexible Bi_2O_2Se transistors after 0, 200, 400, ..., 1000 consecutive bending cycles at a 4.0 mm bending radius. (f) Field-effect mobilities of the device as a function of bending cycles.

of Bi-containing precursors enables its facile thickness control of Bi_2O_2Se thin film down to a few atomic layers just by changing the rotation speed. The integration of a high-mobility thin-film semiconductor, excellent stability, and easy transfer onto flexible substrates make Bi_2O_2Se a competitive candidate for future flexible electronics.

■ ASSOCIATED CONTENT

Supporting Information

The Supporting Information is available free of charge at https://pubs.acs.org/doi/10.1021/jacs.9b11668.

Experimental details and supplementary figures (PDF)

■ AUTHOR INFORMATION

Corresponding Authors

Jinxiong Wu – *Center for Nanochemistry, Beijing Science and Engineering Center for Nanocarbons, Beijing National Laboratory for Molecular Sciences, College of Chemistry and Molecular Engineering, Peking University, Beijing 100871, China; Tianjin Key Lab for Rare Earth Materials and Applications, Center for Rare Earth and Inorganic Functional Materials, School of Materials Science and Engineering, National Institute for Advanced Materials, Nankai University, Tianjin 300350, China*; Email: jxwu@nankai.edu.cn

Hailin Peng – *Center for Nanochemistry, Beijing Science and Engineering Center for Nanocarbons, Beijing National Laboratory for Molecular Sciences, College of Chemistry and Molecular Engineering, Peking University, Beijing 100871, China*; orcid.org/0000-0003-1569-0238; Email: hlpeng@pku.edu.cn

Authors

Congcong Zhang – *Center for Nanochemistry, Beijing Science and Engineering Center for Nanocarbons, Beijing National Laboratory for Molecular Sciences, College of Chemistry and Molecular Engineering, Peking University, Beijing 100871, China*

Yuanwei Sun – *International Center for Quantum Materials, Electron Microscopy Laboratory, School of Physics, Peking University, Beijing 100871, China; Collaborative Innovation Center of Quantum Matter, Beijing 100871, China*

Congwei Tan – *Academy for Advanced Interdisciplinary Studies, Peking University, Beijing 100871, China*

Tianran Li – *Center for Nanochemistry, Beijing Science and Engineering Center for Nanocarbons, Beijing National Laboratory for Molecular Sciences, College of Chemistry and Molecular Engineering, Peking University, Beijing 100871, China*

Teng Tu – *Center for Nanochemistry, Beijing Science and Engineering Center for Nanocarbons, Beijing National Laboratory for Molecular Sciences, College of Chemistry and Molecular Engineering, Peking University, Beijing 100871, China*

Yichi Zhang – *Center for Nanochemistry, Beijing Science and Engineering Center for Nanocarbons, Beijing National Laboratory for Molecular Sciences, College of Chemistry and Molecular Engineering, Peking University, Beijing 100871, China*

Yan Liang – *Center for Nanochemistry, Beijing Science and Engineering Center for Nanocarbons, Beijing National Laboratory for Molecular Sciences, College of Chemistry and Molecular Engineering, Peking University, Beijing 100871, China*

Xuehan Zhou – *Center for Nanochemistry, Beijing Science and Engineering Center for Nanocarbons, Beijing National Laboratory for Molecular Sciences, College of Chemistry and Molecular Engineering, Peking University, Beijing 100871, China*

Peng Gao – *International Center for Quantum Materials, Electron Microscopy Laboratory, School of Physics, Peking University, Beijing 100871, China; Collaborative Innovation Center of Quantum Matter, Beijing 100871, China;* orcid.org/0000-0003-0860-5525

Complete contact information is available at: https://pubs.acs.org/10.1021/jacs.9b11668

Notes

The authors declare no competing financial interest.

■ ACKNOWLEDGMENTS

We acknowledge financial support from the National Natural Science Foundation of China (21920102004, 21733001, and 21525310), the National Basic Research Program of China

(2016YFA0200101), the National Key R&D Program of China (2016YFA0300804), Beijing National Laboratory for Molecular Sciences (BNLMS201914), the National Natural Science Foundation of China (Grant Nos. 11974023 and 51672007), and the Key R&D Program of Guangdong Province (2018B030327001 and 2018B010109009). We gratefully acknowledge Electron Microscopy Laboratory in Peking University for the use of a Cs-corrected electron microscope.

REFERENCES

(1) Li, L.; Yu, Y.; Ye, G.; Ge, Q.; Ou, X.; Wu, H.; Feng, D.; Chen, X.; Zhang, Y. Black Phosphorus Field-effect Transistors. *Nat. Nanotechnol.* **2014**, *9* (5), 372−7.

(2) Bandurin, D. A.; Tyurnina, A. V.; Yu, G. L.; Mishchenko, A.; Zólyomi, V.; Morozov, S. V.; Kumar, R. K.; Gorbachev, R. V.; Kudrynskyi, Z. R.; Pezzini, S. High electron mobility, quantum Hall effect and anomalous optical response in atomically thin InSe. *Nat. Nanotechnol.* **2017**, *12* (3), 223−227.

(3) Wu, J.; Yuan, H.; Meng, M.; Chen, C.; Sun, Y.; Chen, Z.; Dang, W.; Tan, C.; Liu, Y.; Yin, J.; Zhou, Y.; Huang, S.; Xu, H. Q.; Cui, Y.; Hwang, H. Y.; Liu, Z.; Chen, Y.; Yan, B.; Peng, H. High electron mobility and quantum oscillations in non-encapsulated ultrathin semiconducting Bi_2O_2Se. *Nat. Nanotechnol.* **2017**, *12* (6), 530−534.

(4) Akinwande, D.; Huyghebaert, C.; Wang, C. H.; Serna, M. I.; Goossens, S.; Li, L. J.; Wong, H. P.; Koppens, F. H. L. Graphene and two-dimensional materials for silicon technology. *Nature* **2019**, *573* (7775), 507−518.

(5) Zhang, H.; Cheng, H. M.; Ye, P. 2D nanomaterials: beyond graphene and transition metal dichalcogenides. *Chem. Soc. Rev.* **2018**, *47* (16), 6009−6012.

(6) Liu, Y.; Duan, X.; Huang, Y.; Duan, X. Two-dimensional transistors beyond graphene and TMDCs. *Chem. Soc. Rev.* **2018**, *47* (16), 6388−6409.

(7) Chhowalla, M.; Jena, D.; Zhang, H. Two-dimensional semiconductors for transistors. *Nat. Rev. Mater.* **2016**, *1*, 1−15.

(8) Manzeli, S.; Ovchinnikov, D.; Pasquier, D.; Yazyev, O. V.; Kis, A. 2D transition metal dichalcogenides. *Nat. Rev. Mater.* **2017**, *2* (8) DOI: 10.1038/natrevmats.2017.33.

(9) Fu, Q.; Zhu, C.; Zhao, X.; Wang, X.; Chaturvedi, A.; Zhu, C.; Wang, X.; Zeng, Q.; Zhou, J.; Liu, F.; Tay, B. K.; Zhang, H.; Pennycook, S. J.; Liu, Z. Ultrasensitive 2D Bi_2O_2Se Phototransistors on Silicon Substrates. *Adv. Mater.* **2019**, *31* (1), No. e1804945.

(10) Pi, L.; Li, L.; Liu, K.; Zhang, Q.; Li, H.; Zhai, T. Recent Progress on 2D Noble-Transition-Metal Dichalcogenides. *Adv. Funct. Mater.* **2019**, *1904932*, 1−22.

(11) Akinwande, D.; Petrone, N.; Hone, J. Two-dimensional flexible nanoelectronics. *Nat. Commun.* **2014**, *5*, 5678.

(12) Hong, Y. K.; Liu, N.; Yin, D.; Hong, S.; Kim, D. H.; Kim, S.; Choi, W.; Yoon, Y. Recent progress in high-mobility thin-film transistors based on multilayer 2D materials. *J. Phys. D: Appl. Phys.* **2017**, *50* (16), 164001.

(13) Franklin, A. D. Nanomaterials in transistors: From high-performance to thin-film applications. *Science* **2015**, *349* (6249), aab2750.

(14) Bhimanapati, G. R.; Lin, Z.; Meunier, V.; Jung, Y.; Cha, J. J.; Das, S.; Xiao, D.; Son, Y.; Strano, M. S.; Cooper, V. R. Recent Advances in Two-Dimensional Materials Beyond Graphene. *ACS Nano* **2015**, *9* (12), 11509−11539.

(15) Yoder, M. A.; Yan, Z.; Han, M.; Rogers, J. A.; Nuzzo, R. G. Semiconductor Nanomembrane Materials for High-Performance Soft Electronic Devices. *J. Am. Chem. Soc.* **2018**, *140* (29), 9001−9019.

(16) Watts, M. C.; Picco, L.; Russell-Pavier, F. S.; Cullen, P. L.; Miller, T. S.; Bartus, S. P.; Payton, O. D.; Skipper, N. T.; Tileli, V.; Howard, C. A. Production of phosphorene nanoribbons. *Nature* **2019**, *568* (7751), 216−220.

(17) Fiori, G.; Bonaccorso, F.; Iannaccone, G.; Pala-cios, T.; Neumaier, D.; Seabaugh, A.; Banerjee, S. K.; Co-lombo, L. Electronics based on two-dimensional materials. *Nat. Nanotechnol.* **2014**, *9* (10), 768−79.

(18) Tan, C.; Tang, M.; Wu, J.; Liu, Y.; Li, T.; Liang, Y.; Deng, B.; Tan, Z.; Tu, T.; Zhang, Y.; Liu, C.; Chen, J. H.; Wang, Y.; Peng, H. Wafer-Scale Growth of Single-Crystal 2D Semiconductor on Perovskite Oxides for High-Performance Transistors. *Nano Lett.* **2019**, *19* (3), 2148−2153.

(19) Chen, P.; Zhang, Z.; Duan, X.; Duan, X. Chemical synthesis of two-dimensional atomic crystals, heterostructures and superlattices. *Chem. Soc. Rev.* **2018**, *47* (9), 3129−3151.

(20) Tao, L.; Chen, K.; Chen, Z.; Chen, W.; Gui, X.; Chen, H.; Li, X.; Xu, J. B. Centimeter-Scale CVD Growth of Highly Crystalline Single-Layer MoS_2 Film with Spatial Homogeneity and the Visualization of Grain Boundaries. *ACS Appl. Mater. Interfaces* **2017**, *9* (13), 12073−12081.

(21) Lin, Z.; Liu, Y.; Halim, U.; Ding, M.; Liu, Y.; Wang, Y.; Jia, C.; Chen, P.; Duan, X.; Wang, C.; Song, F.; Li, M.; Wan, C.; Huang, Y.; Duan, X. Solution-processable 2D semiconductors for high-performance large-area electronics. *Nature* **2018**, *562* (7726), 254−258.

(22) Boandoh, S.; Choi, S. H.; Park, J. H.; Park, S. Y.; Bang, S.; Jeong, M. S.; Lee, J. S.; Kim, H. J.; Yang, W.; Choi, J. Y.; Kim, S. M.; Kim, K. K. A Novel and Facile Route to Synthesize Atomic-Layered MoS_2 Film for Large-Area Electronics. *Small* **2017**, *13* (39),1701306.

(23) Kim, Y. H.; Heo, J. S.; Kim, T. H.; Park, S.; Yoon, M. H.; Kim, J.; Oh, M. S.; Yi, G. R.; Noh, Y. Y.; Park, S. K. Flexible metal-oxide devices made by room-temperature photochemical activation of sol-gel films. *Nature* **2012**, *489* (7414), 128−32.

(24) Xiang, L.; Zhang, H.; Dong, G.; Zhong, D.; Han, J.; Liang, X.; Zhang, Z.; Peng, L.-M.; Hu, Y. Low-power carbon nanotube-based integrated circuits that can be transferred to biological surfaces. *Nat. Electron.* **2018**, *1* (4), 237−245.

(25) Das, S.; Gulotty, R.; Sumant, A. V.; Roelofs, A. All two-dimensional, flexible, transparent, and thinnest thin film transistor. *Nano Lett.* **2014**, *14* (5), 2861−6.

(26) Wu, J.; Qiu, C.; Fu, H.; Chen, S.; Zhang, C.; Dou, Z.; Tan, C.; Tu, T.; Li, T.; Zhang, Y.; Zhang, Z.; Peng, L. M.; Gao, P.; Yan, B.; Peng, H. Low Residual Carrier Con-centration and High Mobility in 2D Semiconducting Bi_2O_2Se. *Nano Lett.* **2019**, *19* (1), 197−202.

(27) Wu, J.; Liu, Y.; Tan, Z.; Tan, C.; Yin, J.; Li, T.; Tu, T.; Peng, H. Chemical Patterning of High-Mobility Semiconducting 2D Bi_2O_2Se Crystals for Integrated Optoelectronic Devices. *Adv. Mater.* **2017**, *29* (44), 1704060.

(28) Choi, M.; Park, Y. J.; Sharma, B. K.; Bae, S. R.; Kim, S. Y.; Ahn, J. H. Flexible active-matrix organic light-emitting diode display enabled by MoS_2 thin-film transistor. *Sci. Adv.* **2018**, *4* (4), No. eaas8721.

(29) Nomura, K.; Ohta, H.; Takagi, A.; Kamiya, T.; Hirano, M.; Hosono, H. Room-temperature fabrication of transparent flexible thin-film transistors using amorphous oxide semiconductors. *Nature* **2004**, *432* (7016), 488−492.

(30) Zhou, L.; Xu, K.; Zubair, A.; Liao, A. D.; Fang, W.; Ouyang, F.; Lee, Y. H.; Ueno, K.; Saito, R.; Palacios, T.; Kong, J.; Dresselhaus, M. S. Large-Area Synthesis of High-Quality Uniform Few-Layer $MoTe_2$. *J. Am. Chem. Soc.* **2015**, *137* (37), 11892−5.

(31) Everaerts, K.; Zeng, L.; Hennek, J. W.; Camacho, D. I.; Jariwala, D.; Bedzyk, M. J.; Hersam, M. C.; Marks, T. J. Printed indium gallium zinc oxide transistors. Self-assembled nanodielectric effects on low-temperature combustion growth and carrier mobility. *ACS Appl. Mater. Interfaces* **2013**, *5* (22), 11884−93.

(32) Petti, L.; Münzenrieder, N.; Vogt, C.; Faber, H.; Büthe, L.; Cantarella, G.; Bottacchi, F.; Anthopoulos, T. D.; Tröster, G. Metal oxide semiconductor thin-film transistors for flexible electronics. *Appl. Phys. Rev.* **2016**, *3* (2), 021303.

(33) Myny, K. The development of flexible integrated circuits based on thin-film transistors. *Nat. Electron.* **2018**, *1* (1), 30−39.

(34) Salvatore, G. A.; Münzenrieder, N.; Barraud, C.; Petti, L.; Zysset, C.; Büthe, L.; Ensslin, K.; Tröster, G. Fabrication and transfer of flexible few-layers MoS_2 thin film transistors to any arbitrary substrate. *ACS Nano* **2013**, *7* (10), 8809−8815.

https://dx.doi.org/10.1021/jacs.9b11668
J. Am. Chem. Soc. 2020, 142, 2726−2731

(35) Tang, J.; Cao, Q.; Tulevski, G.; Jenkins, K. A.; Nela, L.; Farmer, D. B.; Han, S.-J. Flexible CMOS integrated circuits based on carbon nanotubes with sub-10 ns stage delays. *Nat. Electron.* **2018**, *1* (3), 191−196.
(36) Yeo, W. H.; Kim, Y. S.; Lee, J.; Ameen, A.; Shi, L.; Li, M.; Wang, S.; Ma, R.; Jin, S. H.; Kang, Z.; Huang, Y.; Rogers, J. A. Multifunctional epidermal electronics printed directly onto the skin. *Adv. Mater.* **2013**, *25* (20), 2773−8.

https://dx.doi.org/10.1021/jacs.9b11668
J. Am. Chem. Soc. 2020, 142, 2726−2731